

Original Article

Dose Profiles Distribution of 6 MV Linear Accelerator Using Monte Carlo Code System for Optimum Treatment planning in Radiotherapy Department

M.I.A.Koshlaf 1,K.L.Adullatif2

1. Libyan Medical Research Center

2. Department of Biomedical Engineering Libyan Academy

Abstract

Monte Carlo (MC) radiotherapy treatment planning has become practical in medical physics, particularly with the rapid development of computer technology. Requires detailed knowledge of linear medical accelerators (Linacs) beam radiation. In the present work the basic dosimetric properties of the 6-MV photon beam and the Varian Clinic 600CLinac were examined. The dosimetric features of interest are, the absorbed dose from the central axis, beam profiles, photon blockers, electron and positron, mean energy, spectral distribution, and isodose curves. Varian Clinic 600C Linac is simulated using the OMEGA BEAMnrc MC code system. Detailed spectra of phase space profiles of a photon beam with a field of view of 10 cm × 10 cm were modeled, simulated and finally analyzed using BEAMdp. The central axis depth dose curves, dose profiles and isodose curves for photon beams in the aqueous phantom were also recorded and analyzed using the DOSXYZnrc, STATDOSE and DOSXYZ_SHOW code. This study demonstrates that MC can generate phase space data files that can be used to generate accurate MC dose distributions for photon beams produced using a high-powered clinical linear accelerator in a water phantom or in patients for radiotherapy.

Keyword: SPECT, attenuation , scattering ,correction , gamma camera , radiopharmaceutical, photopeak energy, Monte Carlo Computer Code.

Citation. Koshlaf . M.I.A. Dose Profiles Distribution of 6 MV Linear Accelerator Using Monte Carlo Code System for Optimum Treatment planning in Radiotherapy Department

<https://doi.org/10.54361/ljmr.17-13>

Received: 12/02/23accepted: 10/03/23; published: 30/06/23

Copyright ©Libyan Journal of Medical Research (LJMR) 2023. Open Access. Some rights reserved. This work is available under the CC BY license

<https://creativecommons.org/licenses/by-nc-sa/3.0/ig>

Introduction:

In Monte Carlo simulation of high energy medical linear accelerators (Linacs), important components are to be controlled in order to shape the output beam[1-4]. The beam passes through a collimator of heavy metal. Below this collimator there is a flattening filter of tungsten. Ion chamber is positioned to monitor the dose and a quadrant is connected to control the beam optics. A pair of collimator at right angles can be rotated around the axis to give square or rectangle field and all these are mounted in the head to about 50 cm from the source. In conventional external beam radiation therapy, many tumors can be treated with a single field from the front and a single field from the back or with two fields from the opposite sides. The combination of fields helps to uniformly deliver dose across the tumor. Sometimes 3 or 4 fields are used. Occasionally, the gantry of the linear accelerator will rotate during the treatment using what is called arc therapy. In the 3-D Conformal Radiation Therapy, there is an advancement of imaging technology for enhanced images of the body which allow for programming of treatment beams to conform better to the shape of a tumor. By treating with large numbers of beams each shaped with a Multi Leaf Collimator (MLC), radiation dose is delivered uniformly and conformally to the tumor. In recent years, the Intensity Modulated Radiation Therapy (IMRT) is considered as one of the latest advancements in radiation therapy.

This new approach to treatment allows for dose sculpting and even distribution of delivery to avoid critical structures while delivering precise uniform treatment. In this technique, the MLC moves and modulates the radiation as the linac treats the patient [5-9].

In our previous study [10] for radiotherapy treatment planning and others [11-16] for even more complicated non-uniform dose distributions around small radioactive particulate (Hot Particles), MC Electron Gamma Shower (EGS) along with its different tools showed their advancements in dose calculations in general and radiotherapy planning in particular. In the present work, the main objective is to, first, simulate the whole Varian Clinic 600C Linac to produce the phase space file at 100 cm Source to Surface Distance (SSD), just above either the patient or the phantom surface, using BEAMnrc code. The phase space file is a collection of representative pseudo-particles emerging from a radiation therapy treatment source along with their properties that include energy, particle type, position, direction, progeny and statistical weight. Analysis of the phase space were done using BEAMDP code. Second, calculations of the transmitted dose in the water phantom are investigated. The Monte Carlo code system BEAMnrc and DOSXYZnrc were used to model the high energy X-ray linac head and to calculate the transmitted dose in the water

phantom. Analysis of the data were done using BEAMdp, STATDOSE and DOSXYZ_SHOW codes.

Monte Carlo Method:

The Monte Carlo simulation of the linear accelerator is a primary tool in external beam radiotherapy [17-21]. Every pseudo-particle in the phase space file should be scored in such a way that it is recorded only once during the course of passage through the scoring surface (no further recording of the same particle or descendants). A phase space file can take the form of a computer file containing the detailed description of the phase space file particles, i.e., phase space file variables as generated via a Monte-Carlo simulation of the treatment source, or the form of a computer code (event generator) which simulates the treatment source using either a full Monte-Carlo simulation or beam model of the radiation therapy source. The present work focuses on

the general design of the Linac head that produces high energy x-ray beam of 6 MeV. The Varian Clinac 600C Linac components are shown in Figure 1, including the exit window, target, primary collimator, flattening filter, monitor chamber, Y jaws and MLC. PEGS4 (EGS preprocessor) cross-section data for the specific materials in the accelerator were from 700 ICRU PEGS4 data file. Tungsten Target (W700ICRU), Primary Collimator (FE700ICRU), Flattening Filter (FE700ICRU), Monitor chamber as 6 layers of AIR-interspaced aluminized MYLAR (AIR700ICRU, AL700ICRU and MYLAR700ICRU), Aluminized lucite mirror (AL700ICRU and PMMA700ICRU and (AIR700ICRU), JAWS as Secondary collimator (W700ICRU) and SLABS of PMMA light field reticle + AIR to the patient (PMMA700ICRU and AIR700ICRU) were set to produce a 10x10 field at 100 cm SSD.

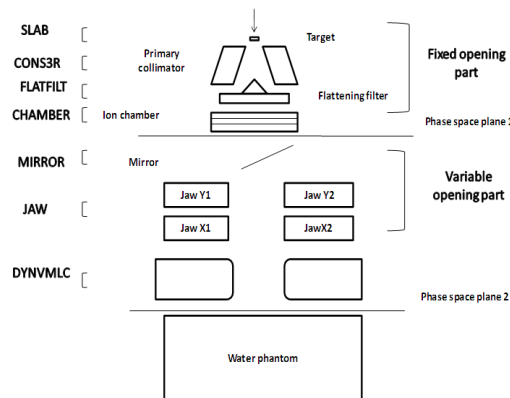


Figure 1: Simulation model of Varian Clinac 600C divided into three main regions: treatment head with fixed opening part up to plane 1, variable opening part between plane 1 and plane 2 and dose calculation inside the water phantom below plane 2.

The simulation was done using DEBIAN GNU Linux 64-bit workstation running a complete Electron Gamma Shower (EGS) Monte Carlo system along with OMEGA-Beam toolkit. The GNU compiler suite c, c++ and Fortran along with the tools TK, TCL, and MAKE were used to compile the codes. DOSXYZ_SHOW was compiled using the Motif development software. All the graphs presented here was done using Grace software for non-linear regression presentation. For all simulations, 2.5×10^7 history were used for creating both the phase space file and scoring the transmitted dose.

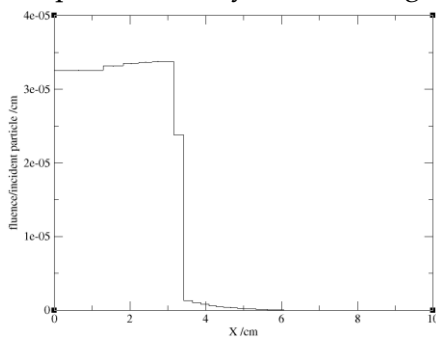
Results and Discussions:

The phase space file at 100 cm SSD where produced by simulating

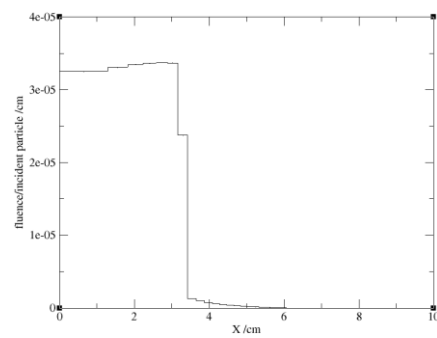
Varian Clinic 600C Linac using BEAMnrc. Beam characteristics data were extracted, analyzed using BEAMdp code and represented to show the following:

Particle Fluence:

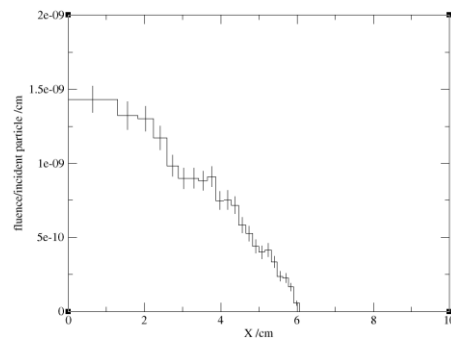
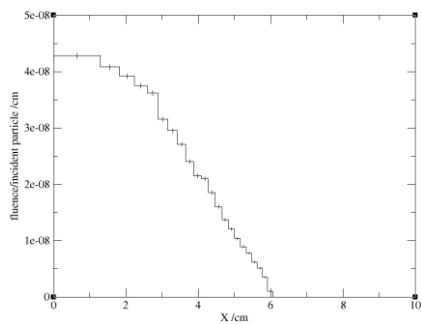
Figure 2 shows the particle fluence versus position x for; all particles (a), photons (b), electrons (c) and positrons (d). All the graphs shows the same trend except that the number of electrons and positrons are quite low compared to the number of photons. This is quite clear from the y-axis scales where the beam is in fact photons with some electrons and positrons scattered from the collimating parts. Notice the high standard deviation in the positron graph due to its poor count rate statistics.



(a)



(b)



(c)

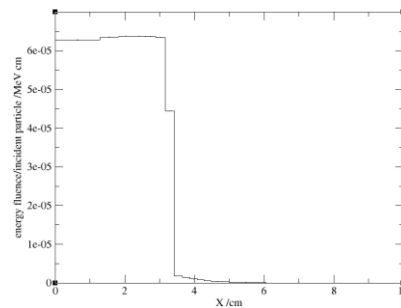
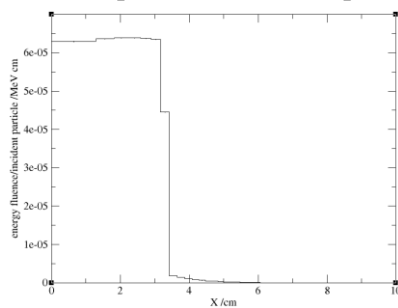
(d)

Figure 2: Total (a), photon (b), electron (c) and positron (d) fluence are represented as functions of distance x .

Energy Fluence:

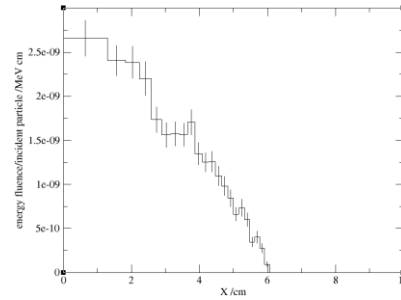
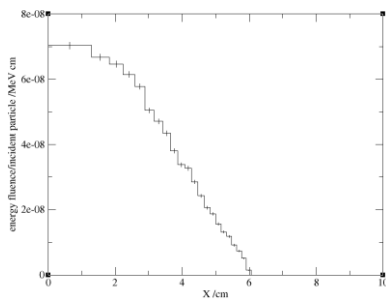
Figure 4 shows the particle energy fluence versus position x for; all particles (a), photons (b), electrons (c) and positrons (d). All the graphs shows again the same trend except that the number of electrons and positrons are quite low compared to the number of photons. This is quite

clear from the y-axis scales where the beam is in fact photons with some electrons and positrons scattered from the collimating parts. Notice the high standard deviation in the positron graph due to its poor count rate statistics.



(a)

(b)



(c)

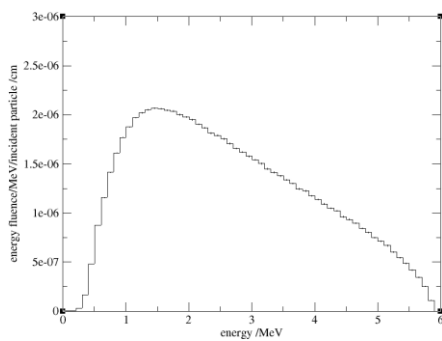
(d)

Figure 3: Total (a), photon (b), electron (c) and positron (d) energy fluence are represented as functions of distance x .

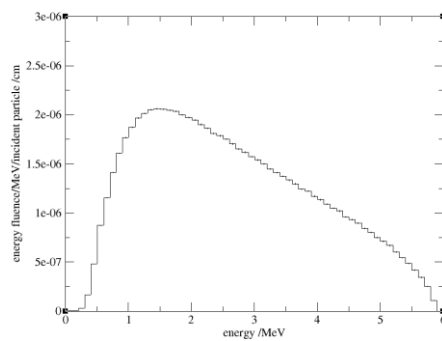
Energy Fluence Distribution:

Figure 4 shows the particle energy fluence distribution for; all particles (a), photons (b), electrons (c) and positrons (d). All the particles were scored in energy bins and the graphs show again the same trend except that the number of electrons and positrons are quite low compared to

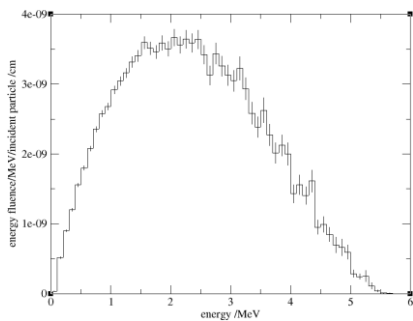
the number of photons. This is quite clear from the y-axis scales where the beam is in fact photons with some electrons and positrons scattered from the collimating parts. Notice the high standard deviation in the positron graph due to its poor count rate statistics.



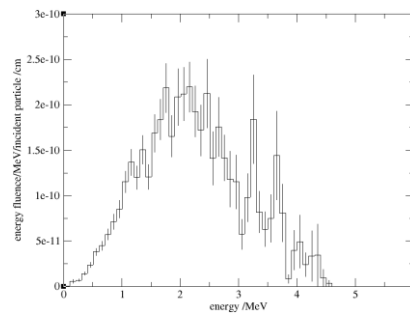
(a)



(b)



(c)



(d)

Figure 4: Total (a), photon (b), electron (c) and positron (d) energy fluence distribution are represented as functions of energy bins.

Angular Distribution:

Figure 5 shows the particle angular distribution for; all particles (a), photons (b), electrons (c) and positrons (d). All the particles were scored in angular bins and the graphs

do not show the same trend where there are a number of electrons and positrons are scattered by the collimator parts with angles

sometimes reach 30o-40o compared to about 4o angles of photons.

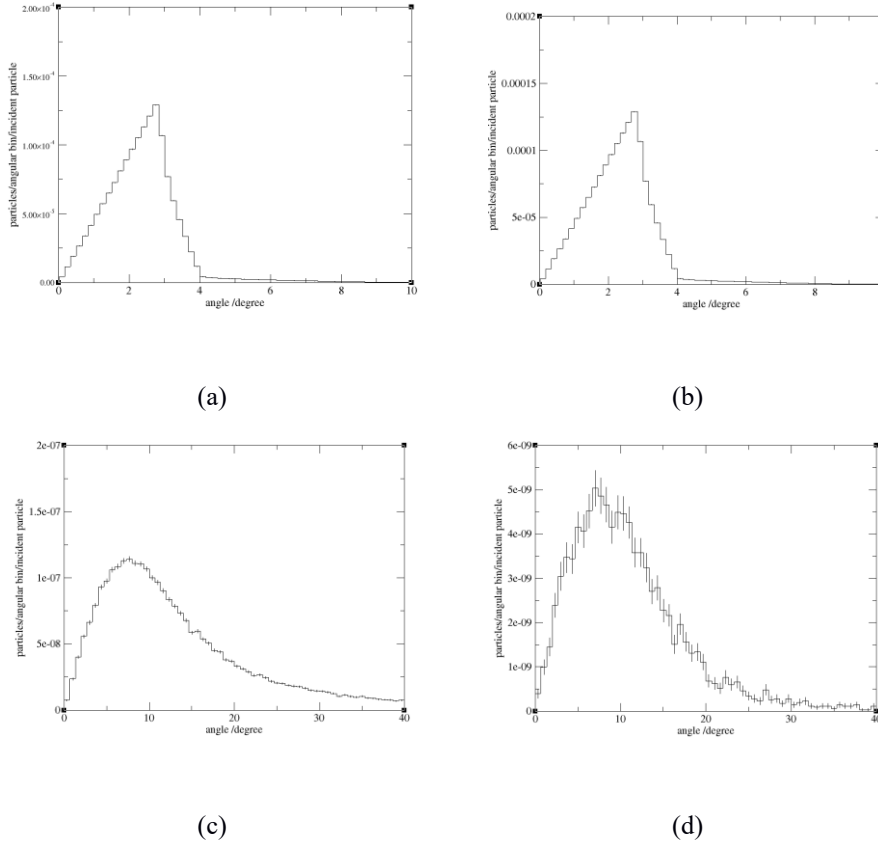


Figure 5: Total (a), photon (b), electron (c) and positron (d) angular distribution are represented as functions of angle degree.

Mean Energy:

Figure 6 shows the particle mean energy versus position x for; all particles (a), photons (b), electrons (c)

and positrons (d). where the mean energy is highest at the center of the beam for all particles.

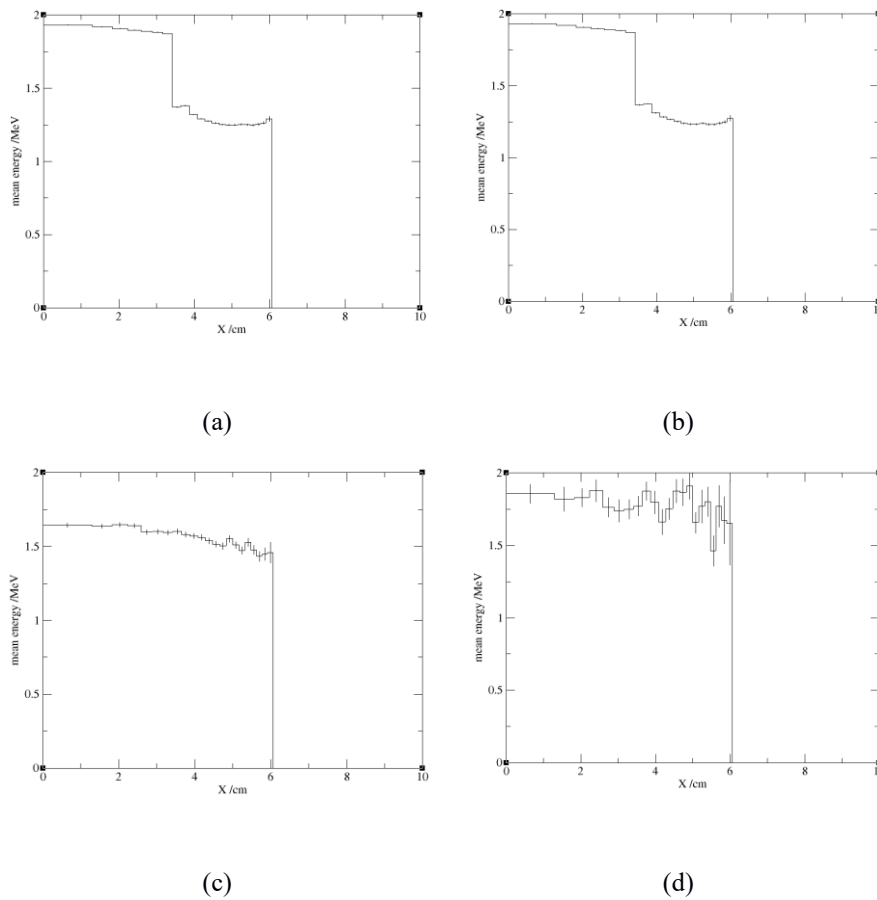


Figure 6: Total (a), photon (b), electron (c) and positron (d) mean energy are represented as functions of distance x .

Spectral Distribution: The phase space file were used to obtain the spectral distribution of 10cmx10cm field of view beam as shown in Figure 7. The figure shows that the photons are the main component of the beam and the least are the electrons and positrons. The less is the number of either electrons or positrons in the produced beam, the higher is the scattering of points of the spectral curve. This is due to the poor statistics of the very small number of electrons and even more for positrons. This is expected for a photon beam of any linear accelerator

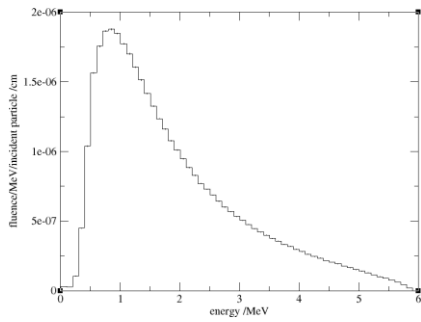
because of the interactions of the emerging x-ray photons with the collimators.

Depth Dose Distributions and Dose Profiles:

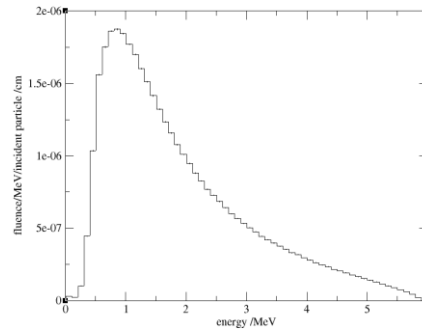
The phase space file was used to score the depth dose distribution curves in the water phantom at 100cm SSD using the DOSXYZnrc code system. The data were analyzed and presented using STATDOSE code with the aid of Grace software. Figure 8(a) shows the dose curves at three different xy plane areas in the direction off the central axis where the depth is set in the z-direction. The

maximum dose D_{max} moves toward higher depths as the xy area increases. Figure 8(b) shows the dose profile of the beam around the central

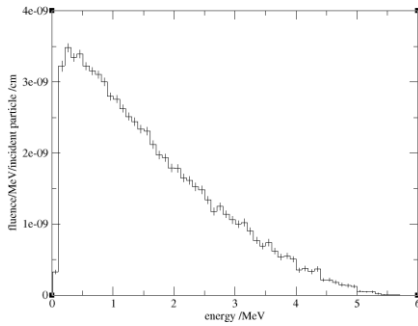
axis. It shows the dose fall off at 5cm on either side which is the radius of the 10cmx10cm field of view of the photon beam.



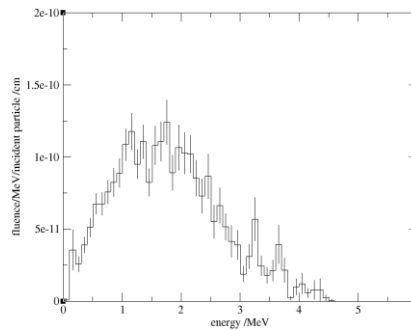
(a)



(b)

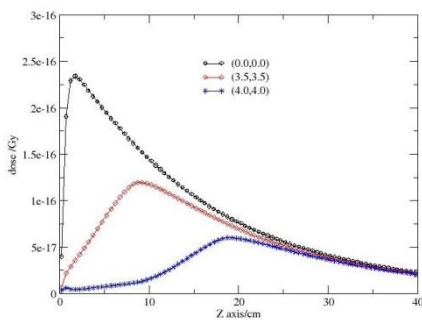


(c)

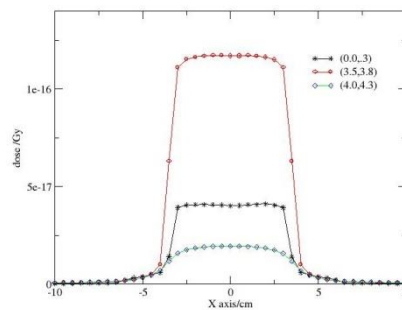


(d)

Figure 7: Total (a), photon (b), electron (c) and positron (d) spectral distribution are represented as functions of energy bins.



(a)



(b)

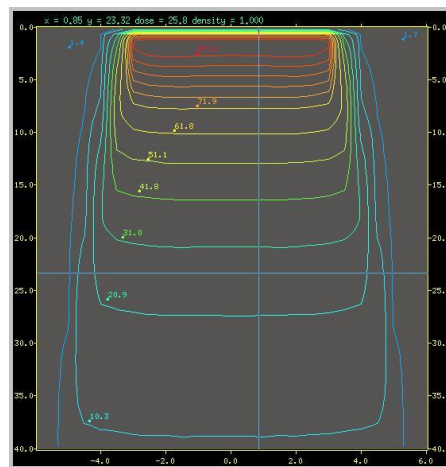
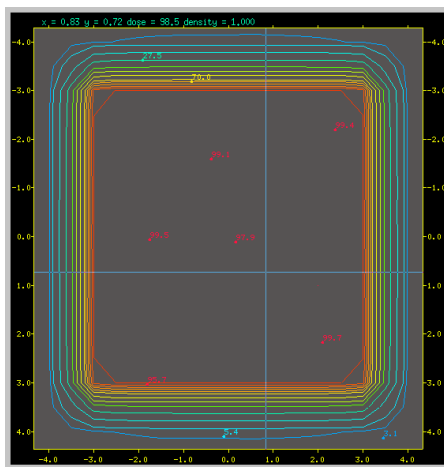
Figure 8: Depth dose distribution of 10cmx10cm photon beam in water phantom (a) and dose profile of the central beam (b).

. Planar and volumetric variations in depth doses are usually displayed Isodose Curves:

The data of the central axis depth doses combined with the dose profiles gives complete 2-D and 3-D information about a radiation beam. This information is difficult to visualize by means of isodose curves or isodose surfaces, which connect points of equal dose in a volume of interest to represent the so-called dose contour. The isodose curves and surfaces are usually drawn at regular intervals of absorbed dose and are expressed as a percentage of the dose at a specific reference point. An isodose chart for a given single beam consists of a family of isodose curves usually drawn at regular increments of Percentage Depth Dose (PDD).

The dose then could be normalized in either Source to Surface Distance set-up (SSD) or in Source to Axis

Distance (SAD) set-up. In the present work, the DOSXYZ_SHOW software was used to display the dose data with the created water phantom file during the simulation. Figure 5 shows the isodose charts for a 6MV linear accelerator x-ray beam in water phantom. It shows an SSD set-up ($A = 10 \times 10 \text{ cm}^2$; $SSD = 100 \text{ cm}$). Figure 9 (a) shows xy planner view while figure 9 (b) is the xz planner view. The coordinate cross markers in both figures can move everywhere at any position on the image to display the dose information at the top of the images. The isodose curves show that near the beam edges in the penumbra region, the dose decreases rapidly with lateral distance from the beam central axis. This dose fall-off is apparently caused by both the geometric penumbra effect and the reduced side scatter.



(a)

(b)

Figure 9: Isodose charts for a 16MV linear accelerator x-ray beam in water phantom. It shows an SSD set-up ($A = 10 \times 10 \text{ cm}^2$; $\text{SSD} = 100 \text{ cm}$). Figure (a) shows xy planner view while figure 9 (b) is the xz planner view

Conclusion:

The Monte Carlo MC code OMEGA BEAM was used to simulate the Varian Clinic 600C Linac using BEAMnrc photon beam linear accelerator. The accelerator beam spectra at 100cm source to surface distance SSD were produced and analyzed. The depth dose curves and dose profiles for 10cmx10cm field of view beam were scored in water

phantom. Planar and volumetric variations in depth doses were displayed by means of isodose curves or isodose surfaces, which connect points of equal dose in a volume of interest to represent the so-called dose contour. OMEGA BEAM code proved to be capable and accurate for radiotherapy treatment planning.

References:

1. Rogers, D. W., W. B., et al. (2007). "BEAMnrc User's Manual." Report PIRS 0509.
2. Rogers, D. W., B. A. Faddegon, et al. (1995). "BEAM: a Monte Carlo code to simulate radiotherapy treatment units." *Med Phys* 22 (5): 503-24.
3. Rogers, D. W., B. Walters, et al. (2004). "DOSXYZnrc User's Manual." Report PIRS 794.
4. Rogers, D. W. O. and A. F. Bielajew (1990). "Monte Carlo Technique of Electron and Photon Transport for Radiation Dosimetry." *The Dosimetry of Ionizing Radiation - Academic Press* 3 : 427-539.
5. Johns, H. E. and J. R. Cunningham (1983). "The
6. van Dyk, J. (1999). "The Modern Technology of Radiation Oncology – A Compendium for Medical Physicists and Radiation Oncologists." Medical Physics Publishing.
7. Khan, F. M. (2003). "The Physics of Radiation Therapy." Lippincott Williams & Wilkins(3 edition).
8. Luis Alberto Vazquez- Quino et al "Monte Carlo modeling of a Novalis TX Varian 6 MV with HD-120 multileaf collimator" *J Applied Clinical Med Phys*, 13(5), 2012
9. Yang J, Li J, Chen L, Price R, McNeeley S, Qin L, et al.

- Dosimetric verification of IMRT treatment planning using Monte Carlo simulations for prostate cancer. *Phys Med Biol* 2005;50(5):869–78.
10. Othman I E et al Hot Particle Dosimetry, Part-III: Enhanced EGSnrcMP Dose Estimates over EGS4 for a $^{106}\text{Ru/Rh}$ Hot Particle, Compared to Measurements using Imaging Photon Detector, RadioChromic Dye Film and Extrapolation Chamber, The Second Symposium on Theories and Applications of Basic and Biosciences 5 September 2015
 11. Othman, I. E., Charles, M. W. and Darley, P. J. "Beta dose measurements and calculations around ^{170}Tm model hot particle using the Monte Carlo code EGS4 and Thermoluminescence Imaging Photon Detector" Intern. Conf. on Advanc. Monte Carlo for Radiat. Phys., Part. Trans. Simulat. and Apps., Lisbon, Portugal 23-26 Oct. (2000).
 12. Darley, P. J., Othman, I. E. and Al-Aydarous, A. Sh., "Dosimetry intercomparisons for ^{106}Ru Hot Particles" University of Birmingham, Radiation Dosimetry Group, PR HPD/00/01 (2000).
 13. Darley, P. J., Othman, I. E. and Al-Aydarous, A. Sh., "Hot Particle Radiation Dosimetry: Development and validation of measurement and calculation techniques" University of Birmingham, Radiation Dosimetry Group, FR HPD/00 (2000).
 14. Adamiec, G. and Othman, I. E. "Evaluation of dose distributions around hot particles by means of TL measurements" The University of Oxford, Research Laboratory for Archaeology and the History of Art, REP; GR-766-310-A (1999).
 15. Darley, P. J., Charles, M. W., Othman, I. E., Al-Aydarous, A. Sh., and Mill, A. J., "Origins and dosimetry of 'hot particles' from nuclear plant operation" *Radiat. Prot. Dosim.* 92 (1-3) 131-137 (2000).
 16. Darley, P. J., Villarreal Barajas, J. E. and Othman, I. E. "Hot Particle Radiation Dosimetry: Development and validation of measurement and calculation techniques for hot particles" University of Birmingham,

- Radiation Dosimetry Group, AR
HPD/99 (1999).
17. Yamamoto T, Mizowaki T, Miyabe Y, Takegawa H, Narita Y, Yano S, et al. An integrated Monte Carlo dosimetric verification system for radiotherapy treatment planning. *Phys Med Biol* 2007;52(7):1991–2008.
 18. Rogers DWO, Faddegon BA, Ding GX, Ma C-M, We J, Mackie TR. BEAM: A Monte Carlo code to simulate radiotherapy treatment units. *Med Phys* 1995;22(5):503–24.
 19. Kawrakow I, Walters BRB. Efficient photon beam dose calculations using DOSXYZnrc with BEAMnrc. *Med Phys* 2006;33(8):3046–56.
 20. Joao Seco and Frank Verhaegen, Monte Carlo Techniques in Radiation Therapy, Editors ISBN: 978-1-4665-0792-0
 21. Chetty et al.: Report of the AAPM Task Group No. 105: Issues associated with clinical implementation of Monte Carlo-based photon and electron external beam treatment planning, *Med. Phys.* 34(12), December 2007.